

Denosing Using Wavelets and Projections onto the ℓ_1 -Ball

June 11, 2014

A. Enis Cetin, M. Tofghi

Dept. of Electrical and Electronic Engineering, Bilkent University, Ankara, Turkey
 cetin@bilkent.edu.tr, tofghi@ee.bilkent.edu.tr

Both wavelet denosing and denosing methods using the concept of sparsity are based on soft-thresholding. In sparsity based denosing methods, it is assumed that the original signal is sparse in some transform domains such as the wavelet domain and the wavelet subsignals of the noisy signal are projected onto ℓ_1 -balls to reduce noise. In this lecture note, it is shown that the size of the ℓ_1 -ball or equivalently the soft threshold value can be determined using linear algebra. The key step is an orthogonal projection onto the epigraph set of the ℓ_1 norm cost function.

In standard wavelet denosing, a signal corrupted by additive noise is wavelet transformed and resulting wavelet subsignals are soft and/or hard thresholded. After this step the denoised signal is reconstructed from the thresholded wavelet subsignals [1, 2]. Thresholding the wavelet coefficients intuitively makes sense because wavelet subsignals obtained from an orthogonal or biorthogonal wavelet filterbank exhibit large amplitude coefficients only around edges or change locations of the original signal. Other small amplitude coefficients should be due to noise. Many other related wavelet denosing methods are developed based on Donoho and Johnstone's idea, see e.g. [1–6]. Most denosing methods take advantage of sparse nature of practical signals in wavelet domain to reduce the noise [7–12].

Consider the following basic denosing framework. Let $v[n]$ be a discrete-time signal and $x[n]$ be a noisy version of $v[n]$:

$$x[n] = v[n] + \xi[n], \quad n = 0, 1, 2, \dots, N - 1. \quad (1)$$

where $\xi[n]$ is the additive, i.i.d, zero-mean, white Gaussian noise with variance σ^2 . An L-level discrete wavelet transform of $x[n]/\sqrt{N}$ is computed and the lowband signal x_L and wavelet subsignals w_1, w_2, \dots, w_L are obtained as shown in Fig. 1. After this step, wavelet subsignals are soft-thresholded as shown in Fig. 2. The soft threshold, θ_i , can be selected in many ways. One possible choice is

$$\theta_i = \gamma \cdot \sigma \cdot \sqrt{2 \log(N)/N}, \quad (2)$$

where γ is a constant [2]. The problem with this threshold is that the noise variance σ^2 has to be known or properly estimated from the observations, $x[n]$.

Another way to denoise the wavelet subsignals w_1, w_2, \dots, w_L is to project them onto ℓ_1 -balls. As pointed out above denosing is possible with the assumption that wavelet subsignals are also sparse signals. Projection $w_{pi}[n]$ of $w_i[n]$ onto an ℓ_1 -ball is obtained as follows:

$$w_{pi} = \operatorname{argmin} \|w_i - w\|_2^2 \quad (3)$$

$$\text{such that } \sum_n |w[n]| \leq d_i,$$

where d_i is the size of the i -th ℓ_1 -ball. This minimization problem was studied by many researchers and computationally efficient algorithms were developed (see e.g., [11]). The projection vector w_{pi} is basically obtained by soft-thresholding as in ordinary wavelet denosing. After orthogonal projection onto an ℓ_1 -ball each wavelet coefficient is modified as follows:

$$w_{pi}[n] = \operatorname{sign}(w_i[n]) \cdot \max\{|w_i[n]| - \theta_i, 0\}, \quad (4)$$

where θ_i is a constant whose value is determined according to the size of the ℓ_1 -ball, d_i , as described in Algorithm 1. Equation 4 is basically soft-thresholding with θ_i as the threshold value. Other computationally efficient algorithms capable of computing the projection vector w_{pi} in $O(K)$ time are described in [11]. Projection operations onto ℓ_1 -ball will force small valued wavelet coefficients to zero and retain the edges and sharp variation regions of the signal because wavelet subsignals have large amplitudes corresponding to edges in most natural signals. As in standard wavelet denosing methods the low-band subsignal x_L is not processed because x_L is not a sparse signal for most practical signals.

In standard wavelet denoising, noise variance has to be estimated to determine the soft-threshold value. In this case, the size of the ℓ_1 -ball d_i in (3) or equivalently θ_i in (4) has to be estimated. Another parameter that has to be determined in both standard wavelet denoising and the ℓ_1 -ball based denoising is the number of wavelet decomposition levels. In the next two sections we describe how the size of the ℓ_1 -ball and the number of wavelet decomposition levels can be determined.

I. ESTIMATION OF DENOISING THRESHOLDS USING THE EPIGRAPH SET OF ℓ_1 -BALL

The soft-threshold θ_i is related with the size of ℓ_1 -ball as described in Algorithm 1. The size of the ℓ_1 -ball can vary between 0 and $d_{max,i}$ which is determined by the boundary of the ℓ_1 -ball going through the wavelet subsignal $w_i[n]$:

$$d_{max,i} = \sum_n \text{sign}(w_i[n])w_i[n], \quad (5)$$

where $\text{sign}(w_i[n])$ is the sign of $w_i[n]$. Orthogonal projection of $w_i[n]$ onto a ball with $d = 0$ produces an all-zero result. On the other hand, projection of $w_i[n]$ onto a ball with size $d_{max,i}$, does not change $w_i[n]$ because $w_i[n]$ is on the boundary of the ℓ_1 -ball. Therefore, the ball size z must satisfy the inequality $0 < z < d_{max}$, for denoising. This ℓ_1 -ball condition can be expressed as follows:

$$g(\mathbf{w}) = \sum_{k=0}^{K-1} |w[k]| \leq z, \quad (6)$$

where K is the length of the wavelet subsignal $w_i[n]$ and $\mathbf{w} = [w[0], w[1], \dots, w[K-1]]$. This condition corresponds to the epigraph set of the ℓ_1 -ball in \mathbb{R}^{K+1} [7, 10]. In (6) there are \mathbb{R}^{K+1} variables. These are $w_i[0], \dots, w_i[K-1]$, and z . The epigraph set of ℓ_1 -cost function $g(\mathbf{w}) \leq z$ in \mathbb{R}^3 is shown in Fig. 4.

Algorithm 1 Order $(K \log(K))$ algorithm implementing projection onto the ℓ_1 -ball with size d_i .

1: **Inputs:**

A vector $w_i[n]$, $n = 0, 1, \dots, K-1$ and scalar $d_i > 0$

2: **Initialize:**

Sort the entries of $|w_i[n]|$ and obtain the rank ordered sequence

$$\mu_1 \geq \mu_2 \geq \dots \geq \mu_K$$

$$\theta_i = \frac{1}{\rho} \left(\sum_{n=1}^{\rho} \mu_n - d_i \right) \quad (7)$$

such that $\rho = \max\{j \in \{0, 1, 2, \dots, K-1\} :$

$$\mu_j - \frac{1}{j} \left(\sum_{r=1}^j \mu_r - d_i \right) > 0\}$$

3: **Output:**

$$w_{pi}[n] = \text{sign}(w_i[n]) \cdot \max\{|w_i[n]| - \theta_i, 0\}, n = 0, 1, 2, \dots, K-1$$

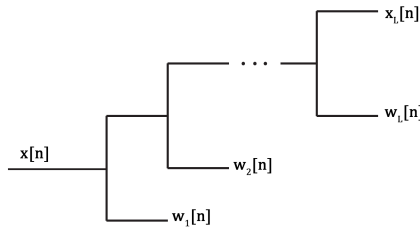


Fig. 1. L-level dyadic wavelet decomposition of the signal x .

By orthogonal projecting the wavelet subsignal $[w_i[n], 0]^T := [w_i[0], \dots, w_i[K-1], 0]^T$ onto the epigraph set it is possible to determine all of the \mathbb{R}^{K+1} unknowns, $w_{pi}[n]$, $n = 0, 1, \dots, K-1$, and

z_p , as graphically illustrated in Fig. 3. The projection vector $[w_{pi}[n], d]^T$ is unique and the closest vector to the wavelet subsignal $[w_i[n], 0]^T$ in \mathbb{R}^{K+1} because the epigraph set is a closed and convex set. The projection onto the epigraph set can be computed in two steps. In the first step, $[w_i[n], 0]^T$ is projected onto the nearest boundary hyperplane of the epigraph set which is

$$\sum_{n=0}^{K-1} \text{sign}(w_i[n]) \cdot w[n] - z = 0. \quad (8)$$

The projection signal $w_{pi}[n]$ onto the hyperplane in \mathbb{R}^{K+1} is determined as follows:

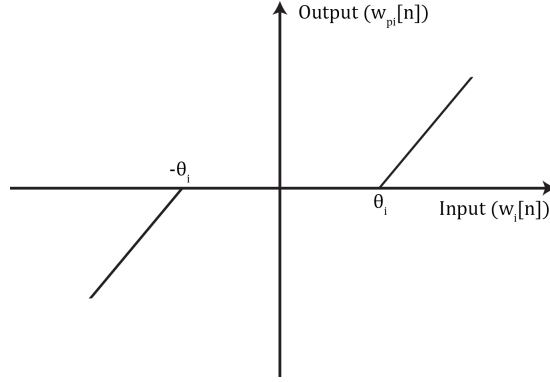


Fig. 2. Soft-thresholding of wavelet coefficients.

$$w_{pi}[n] = w_i[n] + \frac{0 \cdot z - \sum_{n=0}^{K-1} \text{sign}(w_i[n]) w_i[n]}{K+1} \text{sign}(w_i[n]) \quad (9)$$

$$n = 0, 1, \dots, K-1,$$

and

$$z_p = 0 + \frac{\sum_{n=0}^{K-1} \text{sign}(w_i[n]) w_i[n]}{K+1}. \quad (10)$$

This orthogonal projection also determines the size of the ball:

$$d_i = \sum_{n=0}^{K-1} \text{sign}(w_i[n]) w_{pi}[n], \quad (11)$$

because the projection vector $w_{pi}[n]$, $n = 0, 1, \dots, K-1$ must be on the K -dimensional hyperplane with weights $\text{sign}(w_i[n])$. This is graphically illustrated in Fig. 4 (view from the top). The projection $w_{pi}[n]$

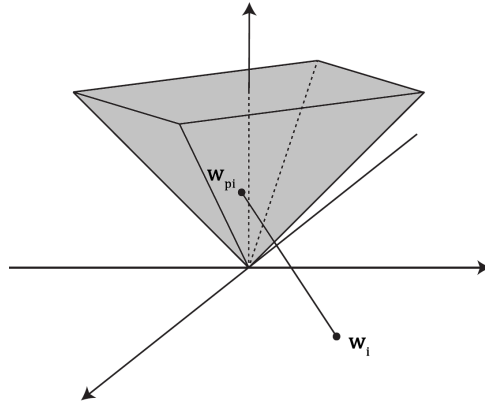


Fig. 3. Projection of $w_i[n]$ onto the epigraph set of ℓ_1 -norm cost function: $z \geq \sum_{n=0}^{K-1} |w[k]|$

may or may not be on the epigraph set of ℓ_1 -ball. If the signs of the projection signal $w_{pi}[n]$ entries are the same as $w_i[n]$ for all n then the $w_{pi}[n]$ is on the epigraph set, otherwise $w_{pi}[n]$ is not on the ℓ_1 -ball as shown in Fig. 4. If $w_{pi}[n]$ is not on the ℓ_1 -ball we can still project $w_i[n]$ onto the ℓ_1 -ball using Algorithm 1 or Duchi et al's ℓ_1 -ball projection algorithm [11] using the values of d_i determined in Eq. (11). This constitutes the second step of epigraph projection operation.

In summary, we have the following two steps: (i) Project $w_i[n]$ onto the boundary hyperplane and determine d_i . (ii) If $sign(w_i[n]) = sign(w_{pi}[n])$ for all n , $w_{pi}[n]$ is the projection vector. Otherwise use d_i value in Algorithm 1 to determine the final projection vector. Vector w_{pi} is the projection of w_i onto the ℓ_1 -ball, but w_{pi} is only the projection of w_1 onto one of the boundary hyperplanes of ℓ_1 -ball.

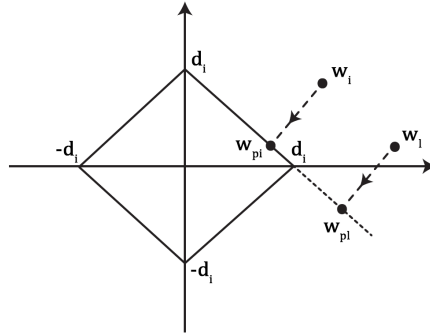


Fig. 4. Orthogonal projection operation onto a bounding hyperplane of ℓ_1 -ball.

II. HOW TO DETERMINE THE NUMBER OF WAVELET DECOMPOSITION LEVELS

It is possible to use the Fourier transform of the noisy signal to estimate the bandwidth of the signal. Once the bandwidth ω_0 of the original signal is approximately determined it can be used to estimate the number of wavelet transform levels and the bandwidth of the low-band signal x_L . In an L -level wavelet decomposition the low-band signal x_L approximately comes from the $[0, \frac{\pi}{2L}]$ frequency band of the signal $x[n]$. Therefore, $\frac{\pi}{2L}$ must be greater than ω_0 so that the actual signal components are not soft-thresholded. Only wavelet subsignals $w_L[n], w_{L-1}[n], \dots, w_1[n]$, which come from frequency bands $[\frac{\pi}{2L}, \frac{\pi}{2L-1}]$, $[\frac{\pi}{2L-1}, \frac{\pi}{2L-2}]$, \dots , $[\frac{\pi}{2}, \pi]$, respectively, should be soft-thresholded in denoising. For example,

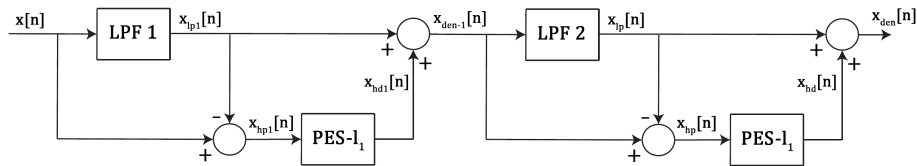


Fig. 5. Pyramidal filtering based denoising. the high-pass filtered signal is projected onto the epigraph set of ℓ_1 .

in Fig. 6, the magnitude of Fourier transform of $x[n]$ is shown for “piece-regular” signal defined in MATLAB. This signal is corrupted by zero-mean white Gaussian noise with $\sigma = 10, 20$, and 30% of the maximum amplitude of the original signal, respectively. For this signal an $L = 3$ level wavelet decomposition is suitable because Fourier transform magnitude approaches to the noise floor level after $\omega_0 = \frac{58\pi}{512}$. It is also a good practice to allow a margin for signal harmonics. Therefore, $(\frac{\pi}{2^3} > \frac{58\pi}{512})$ is selected as the number of wavelet decomposition levels. It is also possible to use a pyramidal structure for signal decomposition instead of the wavelet transform. The noisy signal is low-pass filtered with cut-off frequency $\frac{\pi}{8}$ for “piece-regular” signal and the output $x_{lp}[n]$ is subtracted from the noisy signal $x[n]$ to obtain the high-pass signal $x_{hp}[n]$ as shown in Fig. 5. The signal is projected onto the epigraph of ℓ_1 -ball and $x_{hd}[n]$ is obtained. Projection onto the Epigraph Set of ℓ_1 -ball (PES- ℓ_1), removes the noise by soft-thresholding. The denoised signal $x_{den}[n]$ is reconstructed by adding $x_{hd}[n]$ and $x_{lp}[n]$ as shown in Fig. 5. It is possible to use different thresholds for different subbands as in wavelet transform, using a multisatge pyramid as shown in Fig. 5. In the first stage a low-pass filter with cut-off $\frac{\pi}{2}$ can be used

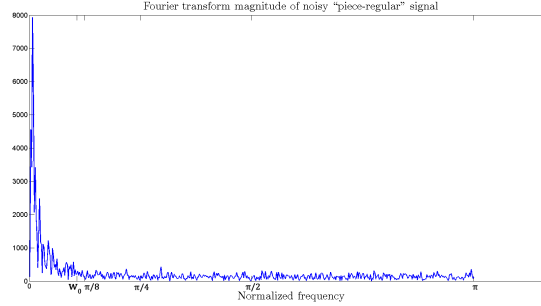


Fig. 6. Discrete-time Fourier transform magnitude of “piece-regular” signal corrupted by noise. The wavelet decomposition level L is selected as 3 to satisfy $\frac{\pi}{2^3} > \omega_0$, which is the approximate bandwidth of the signal.

and $x_{hp1}[n]$ is projected onto the epigraph set of ℓ_1 -ball producing a threshold for the subband $[\frac{\pi}{2}, \pi]$. In the second stage, another low-pass filter with cut-off $\frac{\pi}{4}$ can be used and $x_{hp}[n]$ is projected onto the epigraph set producing a threshold for $[\frac{\pi}{4}, \frac{\pi}{2}]$, etc.

III. SIMULATION RESULTS

Epigraph set based threshold selection is compared with wavelet denoising methods used in MATLAB [2–5]. The “heavy sine” signal shown in Fig. 9(a) is corrupted by a zero mean Gaussian noise with $\sigma = 20\%$ of the maximum amplitude of the original signal. The signal is restored using PES- ℓ_1 with pyramid structure, PES- ℓ_1 with wavelet, MATLAB’s wavelet multivariate denoising algorithm [3, 4], MATLAB’s soft-thresholding denoising algorithm (for “minimaxi” and “rigsure” thresholds), and wavelet thresholding denoising method. The denoised signals are shown in Fig. 9(c), 9(d), 9(e), 9(f), 9(g), and 9(h) with SNR values equal to 23.84, 23.79, 23.52, 23.71, 23.06 dB, and 21.38, respectively. On the average, the proposed PES- ℓ_1 with pyramid and PES- ℓ_1 with wavelet method produce better thresholds than the other soft-thresholding methods. MATLAB codes of the denoising algorithms and other simulation examples are available in the following web-page: <http://signal.ee.bilkent.edu.tr/1DDenoisingSoftware.html>.

Results for other test signals in MATLAB are presented in Table I. These results are obtained by averaging the SNR values after repeating the simulations for 300 times. The SNR is calculated using the formula: $\text{SNR} = 20 \times \log_{10}(\|\mathbf{w}_{orig}\| / \|\mathbf{w}_{orig} - \mathbf{w}_{rec}\|)$. In this lecture note, it is shown that soft-denoising threshold can be determined using basic linear algebra.

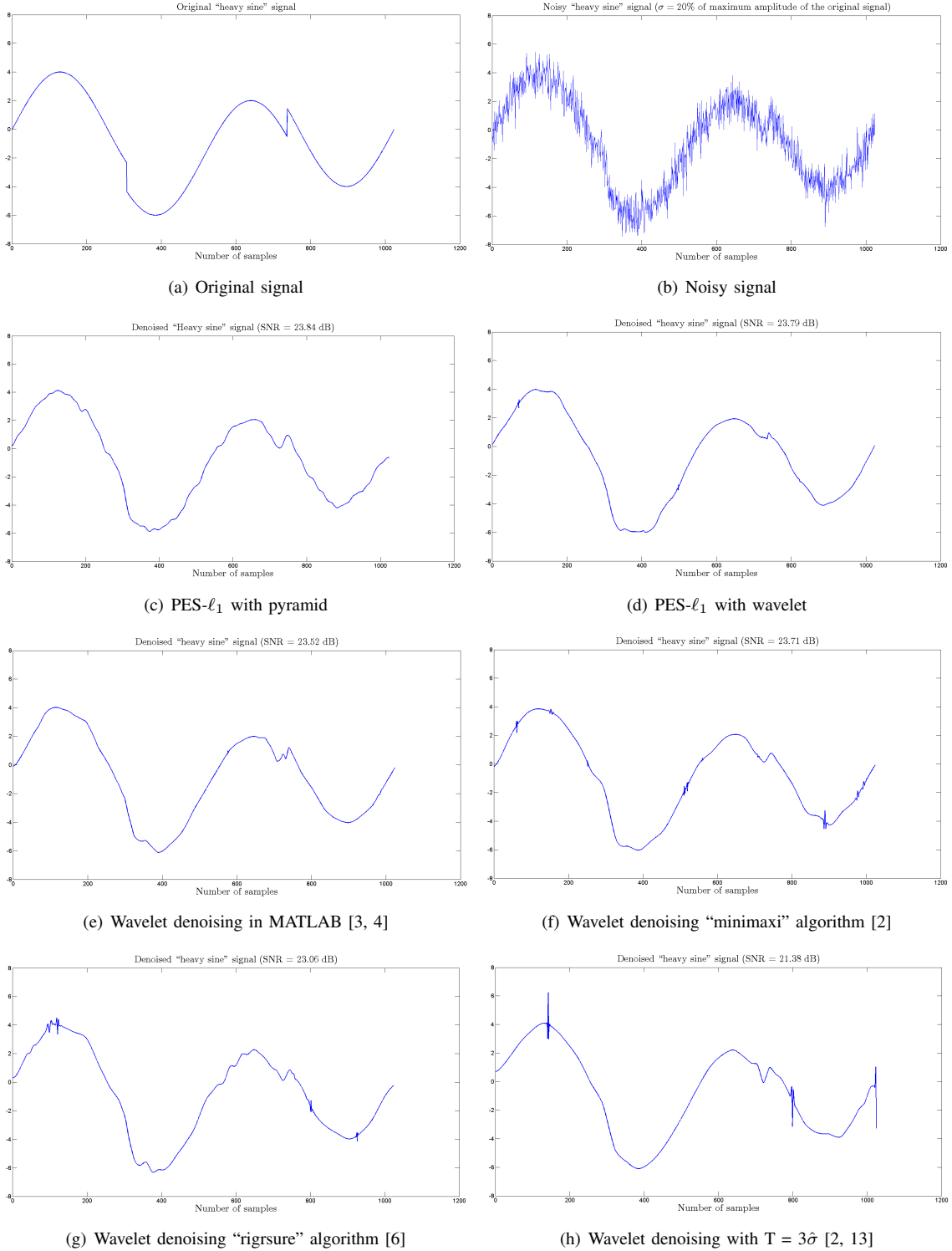


Fig. 7. (a) Original "heavy sine" signal, (b) signal corrupted with Gaussian noise with $\sigma = 20\%$ of maximum amplitude of the original signal, and denoised signal using (c) PES- ℓ_1 -ball with pyramid; SNR = 23.84 dB and, (d) PES- ℓ_1 -ball with wavelet; SNR = 23.79 dB, (e) Wavelet denoising in Matlab; SNR = 23.52 dB [3, 4], (f) Wavelet denoising "minimaxi" algorithm [2]; SNR = 23.71 dB, (g) Wavelet denoising "rigsure" algorithm [6]; SNR = 23.06 dB, (h) Wavelet denoising with $T = 3\hat{\sigma}$ [2, 13]; SNR = 21.38 dB.

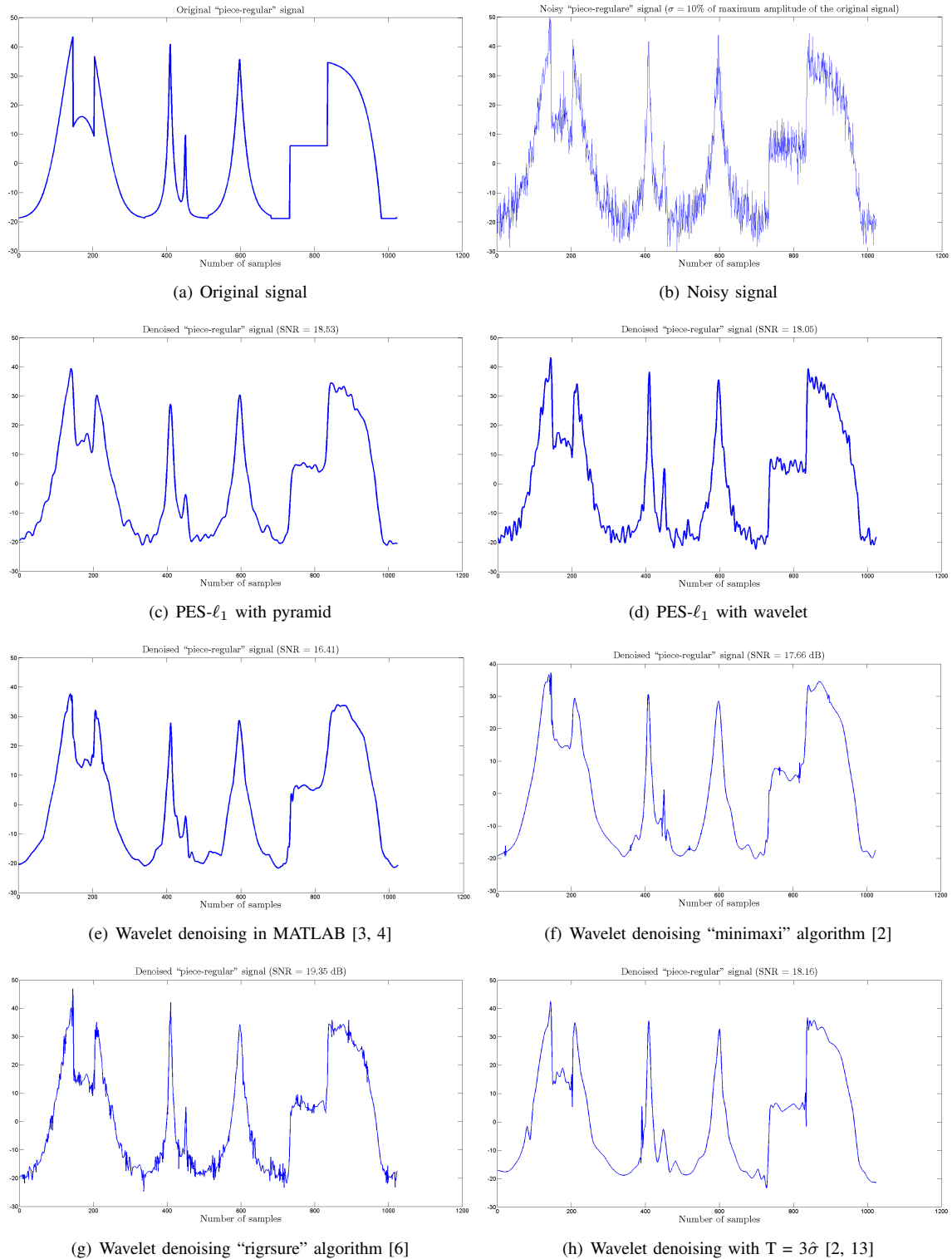


Fig. 8. (a) Original "cusp" signal, (b) signal corrupted with Gaussian noise with $\sigma = 10\%$ of maximum amplitude of the original signal, and denoised signal using (c) PES- ℓ_1 -ball with pyramid; SNR = 23.84 dB and, (d) PES- ℓ_1 -ball with wavelet; SNR = 23.79 dB, (e) Wavelet denoising in Matlab; SNR = 23.52 dB [3, 4], (f) Wavelet denoising "minimaxi" algorithm [2]; SNR = 23.71 dB, (g) Wavelet denoising "rigsure" algorithm [6]; SNR = 23.06 dB, (h) Wavelet denoising with $T = 3\hat{\sigma}$ [2, 13]; SNR = 21.38 dB.

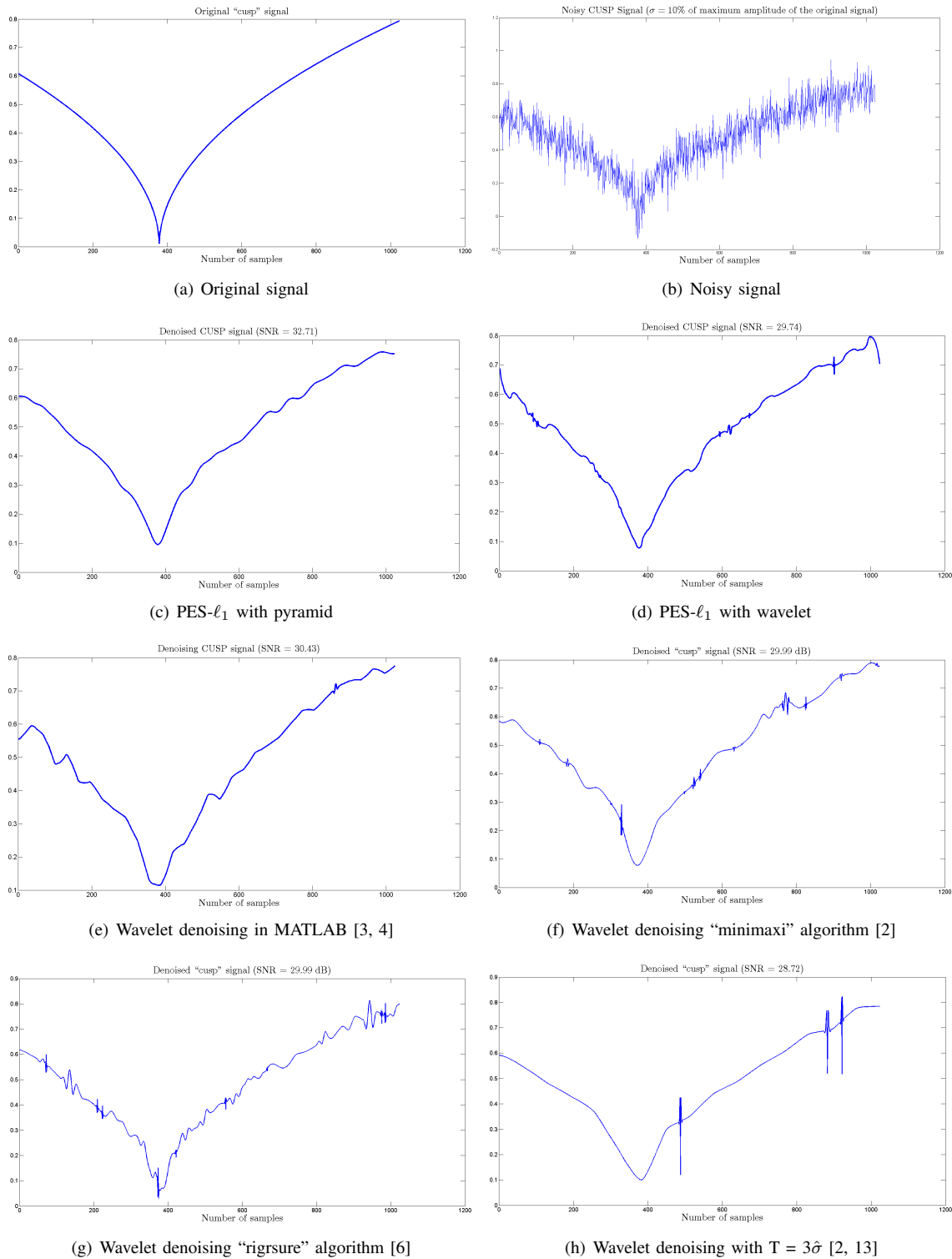


Fig. 9. (a) Original “cusp” signal, (b) signal corrupted with Gaussian noise with $\sigma = 10\%$ of maximum amplitude of the original signal, and denoised signal using (c) PES- ℓ_1 -ball with pyramid; SNR = 23.84 dB and, (d) PES- ℓ_1 -ball with wavelet; SNR = 23.79 dB, (e) Wavelet denoising in Matlab; SNR = 23.52 dB [3, 4], (f) Wavelet denoising “minimaxi” algorithm [2]; SNR = 23.71 dB, (g) Wavelet denoising “rigsure” algorithm [6]; SNR = 23.06 dB, (h) Wavelet denoising with $T = 3\hat{\sigma}$ [2, 13]; SNR = 21.38 dB.

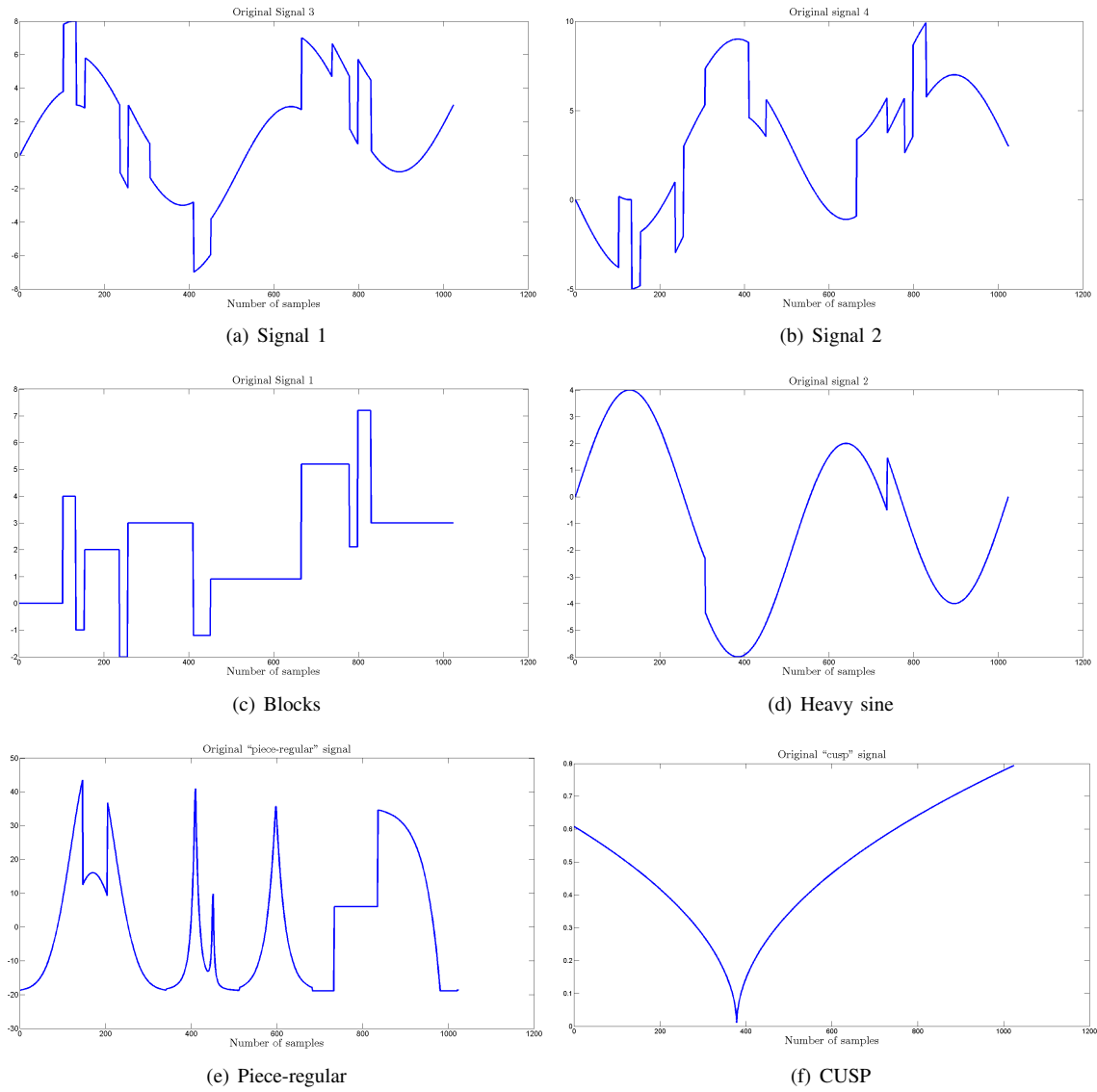


Fig. 10. Signals which are used in the simulations.

TABLE I
COMPARISON OF THE RESULTS FOR DENOISING ALGORITHMS WITH GAUSSIAN NOISE WITH $\sigma = 10, 20, \text{ AND } 30\%$ OF
MAXIMUM AMPLITUDE OF ORIGINAL SIGNAL.

Signal	Input SNR (dB)	PES- ℓ_1 Pyramid	PES- ℓ_1 Wavelet	MATLAB [3, 4]	Soft-threshold $3\hat{\sigma}$	MATLAB "rigsure" [6]	MATLAB "mimimaxi" [2]
Blocks	12.30	17.27	17.08	15.73	17.64	18.32	16.59
Heavy sine	17.77	26.17	26.62	26.87	26.22	27.82	27.75
Signal 1	13.09	18.43	18.10	16.63	17.80	19.18	17.41
Signal 2	13.83	20.37	19.94	18.39	18.92	20.53	19.08
Piece-Regular	12.32	18.53	18.05	16.41	18.16	19.35	17.66
CUSP	16.29	32.58	29.40	30.43	28.72	29.10	29.99
Blocks	6.28	14.34	13.98	12.92	12.87	14.18	13.43
Heavy sine	11.75	23.84	23.79	23.52	21.38	23.06	23.71
Signal 1	7.07	15.70	15.28	14.00	13.30	15.15	14.42
Signal 2	7.80	17.13	17.07	15.84	14.56	16.65	16.20
Piece-Regular	6.27	15.24	14.47	13.11	13.14	14.94	13.99
CUSP	10.25	28.24	24.89	25.04	23.27	23.48	24.44
Blocks	2.76	12.52	12.55	11.37	10.13	12.05	11.64
Heavy sine	9.20	20.89	21.78	21.32	18.79	20.17	21.05
Signal 1	3.56	13.50	13.65	12.37	10.44	13.06	12.72
Signal 2	4.26	15.14	14.25	14.06	12.05	14.37	14.30
Piece-Regular	2.77	13.21	12.70	11.37	9.94	12.43	12.05
CUSP	6.73	25.10	23.47	21.73	19.67	19.69	21.02
Average	9.13	19.68	18.73	17.84	17.06	18.53	18.19

MATLAB CODE

PES- ℓ_1 with pyramid method

In the codes for PES- ℓ_1 with pyramid method, first it starts with loading the original signals as:

```

1 x_orig = zeros(1024,6);
2 load ex4mwden
3 x_orig(:, 5) = load_signal('Piece-Regular', 1024);
4 x_orig(:, 6) = load_signal('cusp', 1024);

```

Then the white Gaussian noise is added as below:

```

1 amp_perc = 0.1;
2 for m = 1:kk
3     sigma(m) = amp_perc*max(x_orig(:, m));
4     NoisySignal(:, m) = x_orig(:, m) + sigma(m)*randn(size(x_orig
5         (:, m)));
6 end

```

which the noise standard deviation is determined with “amp_perc” which in our software it is 0.1, 0.2, and 0.3. Then the iteration number is determined according to the noise power. After all the signal will enter the denoising algorithm which is applied to the noisy signal in “PES_L1_Pyramid.m” function, therefore:

```

1 DenoisedSignal = PES_L1_Pyramid(iter, NoisySignal, kk);

```

which “iter” is the number of the iterations, “NoisySignal” is the corrupted signal, and “kk” is the number of the signals, which here we have six signals in our simulations. In the main function of PES- ℓ_1 denoising “PES_L1_Pyramid.m”, first the signal is passed through the high-pass filter and signal’s high and low frequencies are separated, and then the PES- ℓ_1 algorithm is applied to the high-passed signal. After that, the denoised high-pass signal is added to the unchanged low-pass signal and the main denoised signal is obtained. AS mentioned above, the performance of the algorithms are evaluated by SNR. which are calculated as:

```

1 for d = 1:kk
2     SNR_in(d) = snr(x_orig(:,d), NoisySignal(:,d));
3     SNR_out(d) = snr(x_orig(:,d), DenoisedSignal(:,d));
4 end

```

Since the additive noise is random then we have to run the codes repeatedly for enough times and average them to get the rational SNR value. Which averaging is done as:

```

1 SNR_In_Ave = mean(SNR_in1, 1)
2 SNR_Out_Ave = mean(SNR_out1, 1)

```

Then all the signals (original, noisy, and denoised) are plotted as:

```

1 kp = 0;
2 figure(2)
3 for f = 1:kk
4     subplot(kk,3,kp+1), plot(x_orig(:,f)); axis tight;
5     title(['Original signal', num2str(f)])
6     subplot(kk,3,kp+2), plot(NoisySignal(:,f)); axis tight;
7     title(['Observed signal', num2str(f)])
8     subplot(kk,3,kp+3), plot(DenoisedSignal(:,f)); axis tight;
9     title(['Denoised signal', num2str(f)])
10    kp = kp + 3;
11 end

```

The resulting plot are: and the SNRs are:

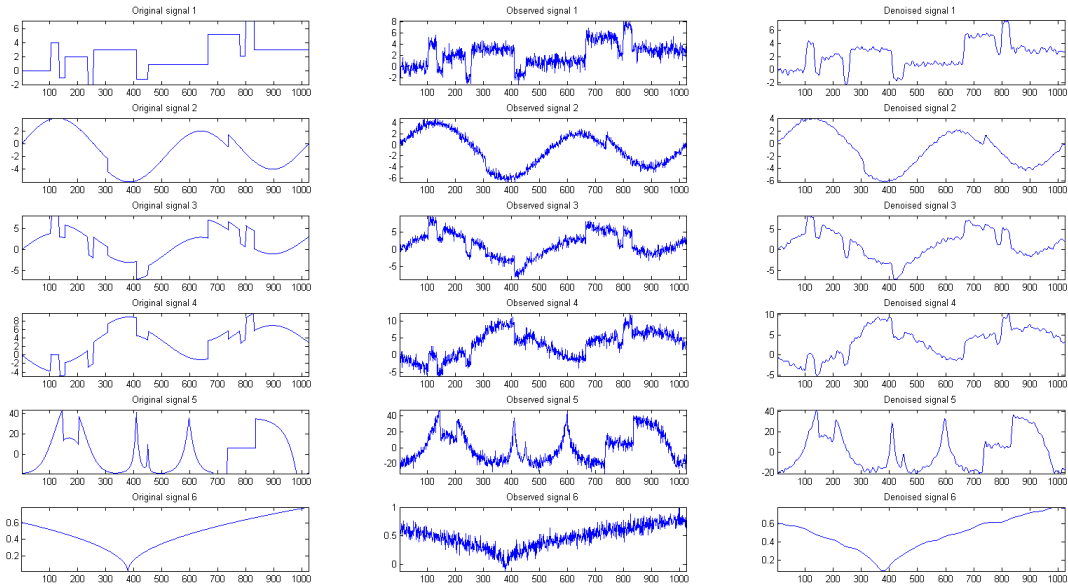


Fig. 11. All the original, noisy, and denoised signals for PES- ℓ_1 with pyramid method.

```

1 SNR_In_Ave =
2
3     6.2994    11.7275    7.0773    7.7911    6.2919    10.2356
4
5
6 SNR_Out_Ave =
7
8     14.3881    23.8448    15.6371    17.1841    15.3298    28.1067
9
10
11 ans =
12
13     19.0818

```

PES- ℓ_1 with wavelet method

All the preliminary steps for this codes are as the same for PES- ℓ_1 with pyramid method. Here, instead of “PES_L1_Pyramid.m”, the function for PES- ℓ_1 with wavelet method “PES_L1_Wavelet.m” is used. In this function the “farras” filter bank is used for wavelet decomposition and the decomposition level is determined as explained in previous sections. It is done as:

```

1     x_dwt1 = circshift(NoisySignal(:, k), f-1); % Shifting the
2           signal
3     [af, sf] = farras; % Wavelet transforms filters
4     J = Jk(k); % Decomposition level
5     x_dwt = dwt_C(x_dwt1, J, af); % Wavelet decomposition

```

then the high subsignals are denoised with PES- ℓ_1 algorithm and the low subsignal is transferred to the output without without any change, then the main denoised signal is reconstructed as follows;

```

1     % Reconstructing the signal from its subsignals
2     im_den(J+1) = x_dwt(J+1);
3     x_idwt1 = idwt_C(im_den, J, sf);
4     x_idwt2(:, f) = circshift(x_idwt1, -f+1); % Shift back

```

again the SNR is calculated as before, and the signals are plotted as follows:

```

1 kp = 0;
2 figure
3 for f = 1:kk
4     subplot(kk,3,kp+1), plot(x_orig(:,f)); axis tight;
5     title(['Original signal ',num2str(f)])
6     subplot(kk,3,kp+2), plot(NoisySignal(:,f)); axis tight;
7     title(['Observed signal ',num2str(f)])
8     subplot(kk,3,kp+3), plot(DenoisedSignal(:,f)); axis tight;
9     title(['Denoised signal ',num2str(f)])
10    kp = kp + 3;
11 end

```

and the SNR values are averaged as before and the signals are plotted as following figure: and the SNRs

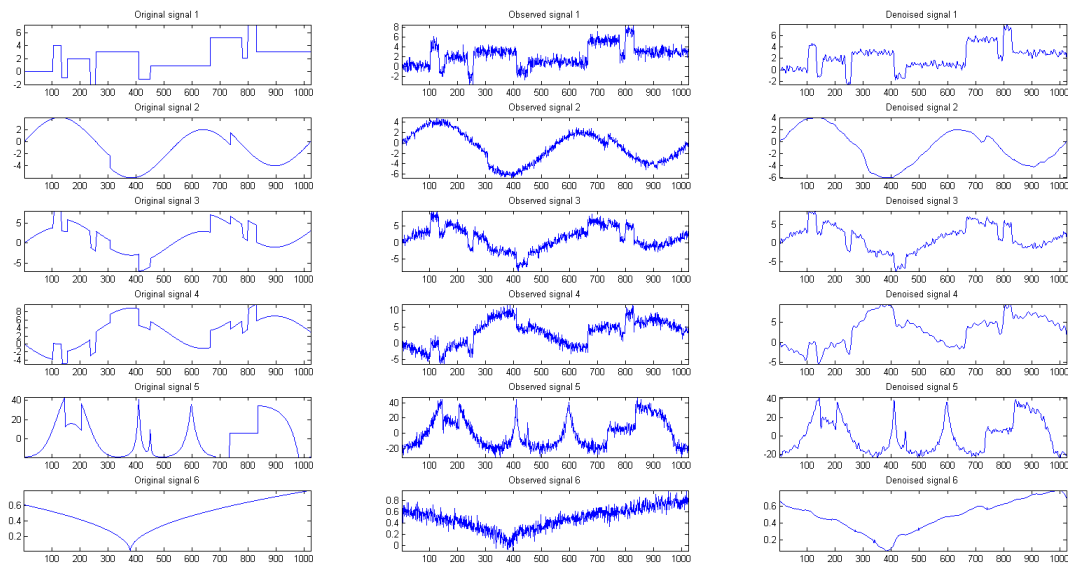


Fig. 12. All the original, noisy, and denoised signals for PES- ℓ_1 with pyramid method.

are:

```

1 SNR_In_Ave =
2
3     6.2991    11.7385    7.0891    7.7825    6.2741    10.2704
4
5
6 SNR_Out_Ave =
7
8     13.9855    23.7737    15.2842    17.0870    14.4843    24.8300
9
10
11 ans =
12
13     18.2408

```

REFERENCES

- [1] S. Mallat and W.-L. Hwang, "Singularity detection and processing with wavelets," *Information Theory, IEEE Transactions on*, vol. 38, no. 2, pp. 617–643, Mar 1992.
- [2] D. Donoho, "De-noising by soft-thresholding," *Information Theory, IEEE Transactions on*, vol. 41, no. 3, pp. 613–627, May 1995.
- [3] M. Aminghafari, N. Cheze, and J.-M. Poggi, "Multivariate denoising using wavelets and principal component analysis," *Computational Statistics and Data Analysis*, vol. 50, no. 9, pp. 2381 – 2398, 2006.
- [4] P. J. Rousseeuw and K. V. Driessen, "A fast algorithm for the minimum covariance determinant estimator," *Technometrics*, vol. 41, no. 3, pp. 212–223, 1999.
- [5] S. Chang, B. Yu, and M. Vetterli, "Adaptive wavelet thresholding for image denoising and compression," *IEEE Transactions on Image Processing*, vol. 9, no. 9, pp. 1532–1546, Sep 2000.
- [6] D. L. Donoho and I. M. Johnstone, "Adapting to unknown smoothness via wavelet shrinkage," *Journal of the American Statistical Association*, vol. 90, no. 432, pp. 1200–1224, 1995.
- [7] G. Chierchia, N. Pustelnik, J.-C. Pesquet, and B. Pesquet-Popescu, "An epigraphical convex optimization approach for multicomponent image restoration using non-local structure tensor," in *IEEE ICASSP, 2013*, 2013, pp. 1359–1363.
- [8] A. E. Cetin, A. Bozkurt, O. Gunay, Y. H. Habiboglu, K. Kose, I. Onaran, R. A. Sevimli, and M. Tofighi, "Projections onto convex sets (POCS) based optimization by lifting," *IEEE GlobalSIP, Austin, Texas, USA*, 2013.
- [9] K. Kose, V. Cevher, and A. Cetin, "Filtered variation method for denoising and sparse signal processing," in *2012 IEEE International Conference on Acoustics, Speech and Signal Processing (ICASSP)*, March 2012, pp. 3329–3332.
- [10] G. Chierchia, N. Pustelnik, J.-C. Pesquet, and B. Pesquet-Popescu, "Epigraphical projection and proximal tools for solving constrained convex optimization problems: Part i," *Arxiv, CoRR*, vol. abs/1210.5844, 2012.
- [11] J. Duchi, S. Shalev-Shwartz, Y. Singer, and T. Chandra, "Efficient projections onto the l_1 -ball for learning in high dimensions," in *Proceedings of the 25th International Conference on Machine Learning*, ser. ICML '08. New York, NY, USA: ACM, 2008, pp. 272–279.
- [12] R. Baraniuk, "Compressive sensing," *IEEE Signal Processing Magazine*, vol. 24, no. 4, pp. 118–121, 2007.
- [13] J. Fowler, "The redundant discrete wavelet transform and additive noise," *IEEE Signal Processing Letters*, vol. 12, no. 9, pp. 629–632, Sept 2005.